Int. J. Electrochem. Sci., 17 **(2022)** Article Number: 220615, doi: 10.20964/2022.06.34

International Journal of
ELECTROCHEMICAL
SCIENCE
www.electrochemsci.org

Short Communication

Trans-1,4-polyisoprene (TPI)) Extracted from Eucommia bark as Natural Corrosion Inhibitor for Carbon Steel in the Simulated Concrete Pore Solution

Chunying Liu

Anhui Vocational And Technical College; Anhui Hefei, 230011 China
E-mail: liucyuta@163.com and liucy@uta.edu.cn

Received: 21 February 2022 / *Accepted:* 29 March 2022 / *Published:* 7 May 2022

The aim of the work was to extract Gutta-percha (trans-1,4-polyisoprene (TPI)) from Eucommia bark and leaves as a natural corrosion inhibitor to inhibit Q235 carbon steel corrosion in a simulated concrete pore solution that contains 3.5wt% NaCl. The results of a SEM study of the surface morphology of steels with and without inhibitors revealed that inhibitor molecules formed a protective layer on the carbon steel surface, which retarded the attack of the Cl^- species and significantly inhibited carbon steel corrosion in a simulated concrete pore solution. EIS and polarization measurements were applied to electrochemical corrosion studies of carbon steel, and results indicated a good agreement between the EIS and polarization studies, which revealed how to enhance the corrosion resistance of Q235 carbon steel with the addition of the TPI as inhibitor in corrosive media. Results showed that the maximum values of corrosion inhibition efficiency were obtained at an average of 85.48% for Q235 carbon steel in the simulated concrete pore solution containing 2.0 g/L of TPI.

Keywords: Carbon Steel; Natural Corrosion Inhibitor; Gutta-Percha; Trans-1,4-Polyisoprene; Electrochemical Impedance Spectroscopy

1. INTRODUCTION

Reinforced concrete is a versatile composite that is widely utilized in modern construction and concrete structure industries like buildings, bridges, highways, and dams [1, 2]. Steel rods, wires, mesh, or cables can be inserted into concrete before it hardens to boost its overall strength and mechanical performance [3-5]. The principal cause of premature steel reinforcement corrosion is chloride ion exposure in reinforced concrete [6, 7]. Chloride ions, which are found in deicing salts and seawater, can promote steel corrosion in reinforced concrete, resulting in increased deflections, fracture widths, and stresses, as well as a reduction in bearing capacity [8, 9].

Corrosion inhibitors are usually chemical compounds added in low concentrations in a corrosive environment to mitigate the corrosion rate of metallic materials when they are in contact with aggressive media [10, 11]. Traditional corrosion inhibitors, on the other hand, are mostly bio-toxic chemical substances with major toxicity issues and are not environmentally benign. Thus, many studies have been performed to identify and optimize environmentally friendly inhibitors [12, 13]. As green corrosion inhibitors, natural products and plant extracts such as ruta graveolens, Argemone mexicana, soya bean, Morinda Lucida, azadirachta, prosopis juliflora, Phyllanthus muellerianus, Bambusa arundinacea, and Vernonia amygdalina, which contain the necessary elements such as O, S, N, and C as active in organic compounds [14, 15].

Gutta-percha, also known as trans-1,4-polyisoprene (TPI), is a polymer of isoprene which is the dominant isomer in natural rubber and has been used in aerospace, medical, chemical, shipbuilding and sports industrials due to its ductility at good insulation, high hardness, room temperature, high anti-impact strength, and alkali and acid corrosion resistance properties [16-18]. Devoting to the study of the green corrosion inhibitors to corrosion inhibition and delay the beginning of corrosion while reducing the corrosion rate, the present study has been first focused on the extraction of TPI from Eucommia bark and leaves as a natural corrosion inhibitor to hinder corrosion of Q235 carbon steel in a simulated concrete pore solution with 3.5 wt% NaCl, a simulating saline or marine environment.

2. EXPERIMENTAL

2.1. Extraction process

According to the presented method in previous reports [19, 20], a thermostatic water (IKA-TRON®ETS-D, IKA Labortechnik) bath and a thermostatic oil bath (ZNCL-GS, Xiaohan (Guangzhou) Trading Co., Ltd., China) were employed for the extraction of TPI from Eucommia bark and leaves. A micro-temperature sensor (103A-11-1M, Hefei Jingpu Sensor Technology Co., Ltd., China) was used to monitor the temperature. A total of 10 g of Eucommia bark and leaf powder were accurately weighed by a digital balance (A&D, Japan) and dried in glass crucibles. The dried powders were dispersed in an 80:10 (by volume) ethanol/turpentine solution in round-bottomed flasks, and the obtained suspension was treated under 12 hours of soaking at 90°C with a 25 mL/g liquid-solid ratio. After cooling, the extracted solution was filtered. In order to obtain crude TPI, the solution was mixed with ethanol and filtered again. The product was stored for 24 hours at 4°C, and subsequently centrifuged at 1000 rpm for 15 minutes. The white precipitates were washed several times with ethanol and dried at 55 °C.

2.2. Preparation simulated concrete pore solution and steel samples

The concrete pore solution was produced by mixing a saturated calcium hydroxide solution (99.995%, Sigma-Aldrich), 0.6 M potassium hydroxide (KOH, 99%, Merck, Germany), 0.2 M sodium hydroxide (NaOH, 99%, Tianjin (FTZ) Junesun Import And Export Co. Ltd., China) with 3.5 wt%

NaCl (99%, Merck, Germany) to simulate marine environment [21, 22]. Different concentrations of TPI (0, 0.3, 0.6, 1.0, and 2.0 g/L) were considered as inhibitors. The Q235 carbon steel in 1 cm in diameter and 10 cm length were washed with distilled water and well-polished with emery paper to reach a bright surface, after carefully welded metallic lead wires, and all the welded joint was sealed with epoxy-resin to certify only working-end-surface of 3mm×3mm size were exposed for test. The steels were rinsed with ethanol and DI water, and dried.

2.3. Electrochemical experiments

The electrochemical impedance spectroscopy (EIS) experiments were carried out at room temperature on a three-electrode system consisting of pretreated steel, saturated calomel electrode (SCE), and a platinum piece as working, reference, and counter electrodes, respectively. Using ac signals at open circuit potential, EIS studies were conducted in the frequency range of 10^{-2}–10^{4} Hz with amplitudes of 7 mV peak-to-peak. ZSimpWin 3.00 PAR software was used to evaluate the data collected. potentiodynamic polarization measurements were made by automatically shifting the electrode potential from -300 to +300 mV against OCP at a 1 mV/s scan rate. For assessment of pitting corrosion behavior, the steel bars were immersed in the simulated concrete pore solution with different concentrations of NaCl (0wt%, 1wt%, 2wt% and 3.5wt%).

2.4. Characterization the steel surface

To study the relevance of the electrochemical results, the steel samples were cut into planchets and the resulting planes of steel discs were pretreated in the same process. All samples were immersed in inhibitor-free solutions and simulated concrete pore solutions with inhibitors for 24 hours. The surface of the samples was studied using scanning electron microscopy (SEM) after they were dried at room temperature.

3. RESULTS AND DISCUSSION

3.1. Electrochemical characterizations

The creation of the passive oxide film, electrolyte, temperature, and corrosion rate all influence the corrosion potential [23]. Figure 1 shows the results of the study the inhibitor concentration effect on the corrosion potential (E_{corr}) of steel in corrosive aqueous solution. It is observed that the E_{corr} of steel samples in the inhibitor-free solution is shifted towards to more negative value (from -0.36 V to -0.52 V). As seen, the shift towards more active values occurs at the beginning of the measurement because of the dissolution of any pre-formed protective oxide layer [24], whereas E_{corr} stabilizes relatively after 4500 s at a value of ~ -0.52 V because of the due establishment of protective oxides and thickening of the oxide film improving its corrosion protection ability [23]. However, it is observed that the presence of inhibitors affects the variation rate of the E_{corr}. E_{corr} has a smaller

variation range than in the inhibitor-free scenario, which could indicate the creation of a protective film of adsorbed species on the metal surface. The thickness of the film thickens as the inhibitor concentration rises, providing additional resistance to mass and charge transfer. As a result, as the concentration increases, the corrosion rate reduces and the inhibitor efficiency rises [25]. After 3000 seconds, the Ecorr value is boosted and subsequently dropped to a stable level. Because of competitive adsorption of ions, the concentration of the corrosive ion to the inhibitor plays a key role in the suppression of localized corrosion [26]. Organic inhibitors, such as TPI, limit localized corrosion by screening the active surface area of the metal through adsorption in preference to hostile ions [27].

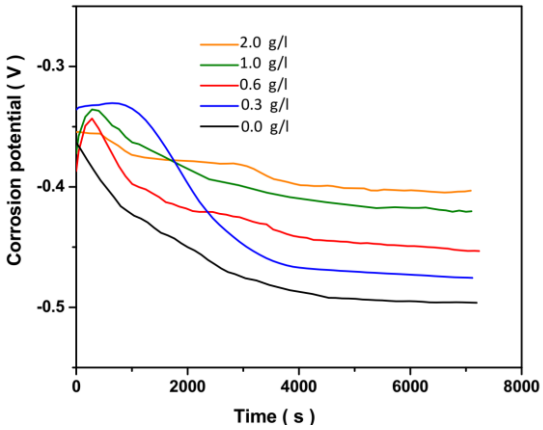

Figure 1. Effect of different concentrations of TPI (0, 0.3, 0.6, 1.0, and 2.0 g/L) as inhibitor on the E_{corr} of Q235 carbon steel in simulated concrete pore solution with 3.5 wt% NaCl

Figure 2 shows the inhibitor concentration effect on the electrochemical impedance response of Q235 carbon steel in the simulated concrete pore solution that contains 3.5wt% NaCl. As can be observed, the Nyquist plots show only one one-time constant corresponding to one capacitive loop, indicating the presence of only one charge transfer mechanism [28, 29]. The diameter of semicircles in the absence and presence of inhibitors is significantly different, signifying that the corrosion process of Q235 carbon steel in 3.5 wt% NaCl simulated concrete pore solution changes after the addition of inhibitors [30, 31]. It is observed that the inhibitor-free solution presents one capacitive semicircle, and the diameter of the semicircle is small. The semicircle diameter is noticeably larger in the presence of inhibitor than in the absence of inhibitor, demonstrating that the addition of TPI effectively retards the migration of corroded particles to the steel surface [32], and indicating TPI's good inhibition performance.

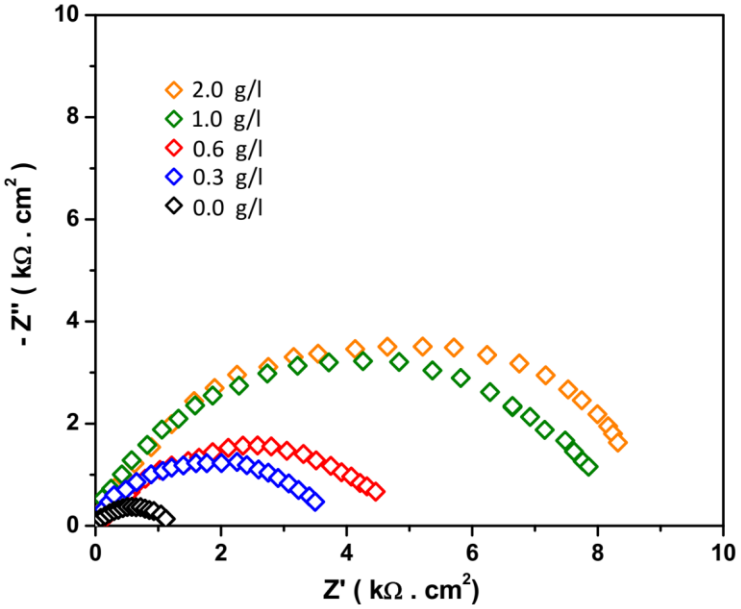

Figure 2. Effect of different concentrations of TPI (0, 0.3, 0.6, 1.0, and 2.0 g/L) as inhibitor on Nyquist plots of Q235 carbon steel in simulated concrete pore solution with 3.5 wt% NaCl in the frequency range of 10^{-2}–10^{4} Hz

Moreover, Figures 3a and 3b show bode plots (phase angle vs. log frequency and log |Z| vs. log frequency). It illustrates that all bode plots have one peak, indicating only one time constant is found in the Bode format. It is revealed that the corrosion of Q235 carbon steel is mainly charge-transfer controlled [33, 34]. The number of phase angle peaks indicates the number of time-constants in general. Furthermore, with the broadening of the peaks, the phase angle shifts upward. The time constant would decrease as a result of this behavior (shifting the phase angle peak toward higher frequencies). It can be associated with the formation of a passive film on the surface of steel, and the enhancement of corrosion resistance [35, 36].

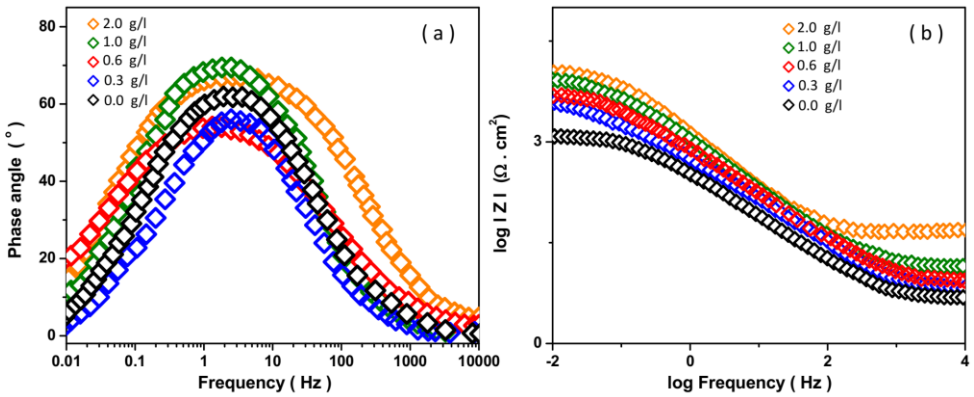

Figure 3. Effect of different concentrations of TPI (0, 0.3, 0.6, 1.0, and 2.0 g/L) as inhibitor on bode plots of Q235 carbon steel in a simulated concrete pore solution that contains 3.5wt% NaCl in the frequency range of 10^{-2}–10^{4} Hz at room temperature; (a) phase angle vs. log frequency and (b) log |Z| vs. log frequency.

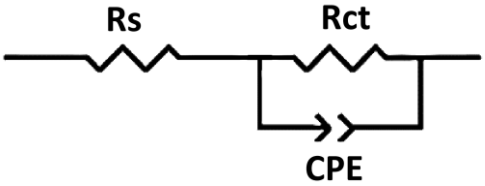

Figure 4. An equivalent circuit model employed to fit the measured impedance data.

Figure 4 depicts an equivalent circuit model that was used to fit the obtained impedance data in order to get the various parameters for describing the metal/solution interface, with CPE presenting a constant phase element for a non-ideal double layer. Rs and Rct stand for solution resistance and charge transfer resistance, respectively. To compensate for variations from ideal dielectric behavior caused by the non-homogeneous nature of the electrode surfaces, the CPE can be employed instead of a capacitor [37, 38]. The admittance and impedance of CPE (Z_{CPE}) are described by the formula [39-41]:

$$Z_{CPE} = \frac{1}{Y_0 (j\omega)^n} \qquad (1)$$

Where Y_0 is the modulus of CPE constant, ω is the angular frequency and n ($0 < n < 1$) is a frequency independent deviation element. When n=1, Z_{CPE} corresponds to an ideal capacitor; n=0 corresponds to an ideal resistor. The inhibition efficiency (IE%) is measured using equation (2):

$$IE\ \% = \frac{R_{ct} - R_{ct}^{o}}{R_{ct}} \times 100 \qquad (2)$$

Where R_{ct} is the charge-transfer resistance while the inhibitor is present, and R_{ct}^{0} presents the charge-transfer resistance when the inhibitor is absent. The obtained parameters are summarized in Table 1 which indicates that the increase in TPI concentration leads to a rise in the Nyquist semicircle radius because it is related to an enhancement of Rct value, which declares the anti-corrosion behavior of TPI.

Table 1. The obtained electrochemical parameters from Nyquist plots

TPI concentration (g/l)	**Rs(Ω.cm^2)**	**Rct(Ω.cm^2)**	**$Y_p \times 10^{-3}$ (s^n/Ω.cm^2)**	**n**	**IE (%)**
0.0	26.51	1139.77	0.71	0.77	—
0.3	33.89	3701.25	0.62	0.79	69.20
0.6	25.96	4751.11	0.29	0.69	76.01
1.0	39.78	8177.21	0.22	0.88	86.06
2.0	13.11	9605.33	0.19	0.80	88.13

Figure 5 shows the potentiodynamic polarization curves of Q235 carbon steel in 3.5 wt% NaCl simulated concrete pore solution with different inhibitor concentrations. The hydrogen evolution reaction is shown on the cathodic branch, whereas the iron dissolution reaction is shown on the anodic branch [42].

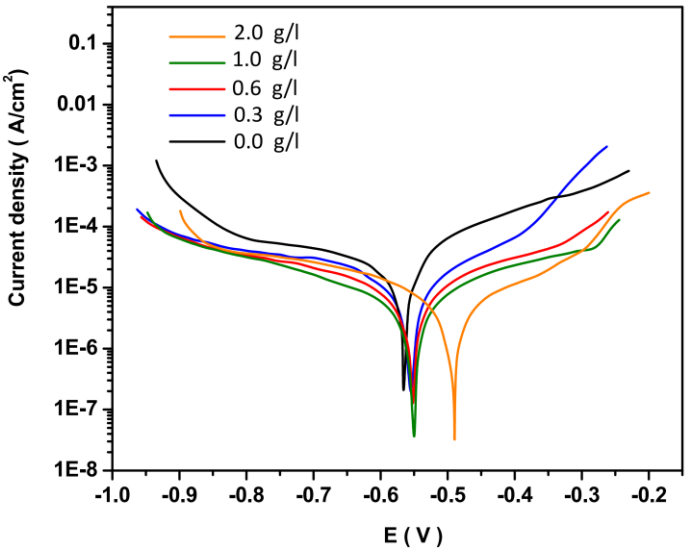

Figures 5. Polarization curves for Q235 carbon steel in a simulated concrete pore solution that contains 3.5wt% NaCl and different concentrations of TPI corrosion inhibitor (0, 0.3, 0.6, 1.0, and 2.0 g/L) at a 1 mV/s scan rate at room temperature.

Table 2. The obtained electrochemical corrosion parameters from potentiodynamic polarization curves

TPI concentration (g/l)	E_{corr}(V)	j_{corr}(μA/cm^2)	R_p(kΩ.cm^2)	CR(mm/year)	IE (%)
0.0	-0.57	20.94	0.360	0.24	—
0.3	-0.55	8.02	9.436	0.09	61.70
0.6	-0.54	5.81	8.297	0.06	72.25
1.0	-0.54	4.22	1.449	0.04	79.84
2.0	-0.50	3.04	6.949	0.03	85.48

The electrochemical corrosion parameters containing the corrosion current density (J_{corr}), corrosion free potential (E_{corr}), the corrosion inhibition efficiency (IE%), and corrosion rate (CR) are calculated from potentiodynamic polarization curves using the following equations [43-46]:

$$IE\ \% = \frac{J^o_{corr} - J_{corr}}{J^o_{corr}} \times 100 \qquad (3)$$

$$CR = \frac{A\, I_{corr}}{n\, F\, \rho} = 0.0116 \times I_{corr} \qquad (4)$$

Where J^{o}_{corr} and J_{corr} show corrosion current densities of carbon steel in the absence and presence of the TPI corrosion inhibitor, respectively. A (55.85 g/mol) and ρ (7.88 g cm^{-3}) are iron atomic weight and density, respectively. F (96485.33 C/mol) is the Faraday constant, and the number of electrons exchanged in the corrosion reaction is denoted by the letter n (n = 2). The obtained electrochemical corrosion parameters are shown in Table 2.

Table 2 displays that as TPI concentration increased, I_{corr} and CR values are decreased and the corrosion inhibition efficiency value is increased. As observed, the maximum values of corrosion inhibition efficiency are obtained at 85.48% for Q235 carbon steel in a simulated concrete pore solution that contains 3.5wt% NaCl and 2.0 g/L concentration of TPI. This shows that the inhibitor molecules are adsorbed on the metal/solution interface, physically shielding the coated area of the metal surface from the corrosive medium's action [47, 48]. The creation of a more stable coating on the electrode surface may account for the increased corrosion protection efficacy at higher concentrations [49-51]. The polyisoprene chains of TPI can be fragmented to obtain oligomers that have reactive chemical groups at their chain ends, therefore they could be modified to insert polymerizable groups [52]. Because oligomers contain more polar groups and have a larger molecular size than monomers, they may cover a larger area on the steel surface and have a better inhibitory effect [53-55]. The results of EIS and polarization measurements are good and indicate an enhancement of the corrosion resistance of Q235 carbon steel in a simulated concrete pore solution that contains 3.5wt% NaCl with the addition of the TPI in corrosive media.

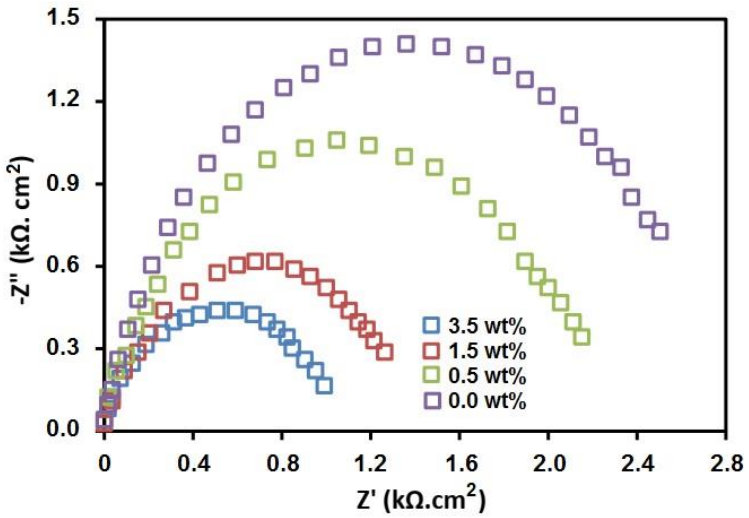

Figure 6. The Nyquist diagrams of carbon steel immersed in the concrete pore solution with different concentrations of NaCl at room temperatures

Figure 6 indicates the Nyquist diagrams of carbon steel immersed in the concrete pore solution with different concentrations of NaCl which revealed a capacitive arc at low frequency. The capacitive arc radius decreases with an increasing concentration values. The semi-circular arc radius in the EIS measurement is related to the polarization resistance of the passive film. A reduction in the overall impedance values with increasing concentration of NaCl reveals a decrease in the corrosion resistance

which is in good accordance with the previous studies. The best fitting parameters based on the circuit depicted in figure 3 are summarized in Table 3. As revealed, the R_{ct} values were considerably reduced from 3045.43Ω to 1139.77Ω for carbon steels, by the addition of NaCl in the concrete pore solution, indicating the chloride presence led to an increase in corrosion on the surface of steel.

Table 3. Electrochemical parameters achieved from the fitted equivalent circuit

NaCl content	R_s (Ω)	R_{ct} (Ω)
Chloride free	27.64	3045.43
0.5wt%	25.83	2334.38
1.5wt%	25.42	1457.94
3.5wt%	26.51	1139.77

3.2. Characterization the steel surface

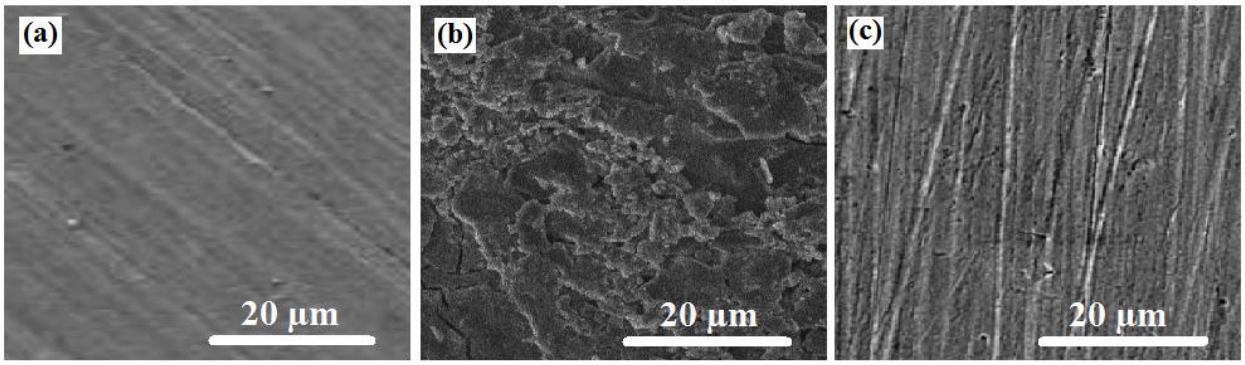

Figure 7. SEM image of (a) as-polished and (b) corroded Q235 carbon steel in a simulated concrete pore solution that contains 3.5wt% NaCl and without inhibitor and (c) with 2.0 g/l concentration of TPI inhibitor solution

The surface morphology of as-polished and corroded Q235 carbon steel in 3.5 wt% NaCl simulated concrete pore solution without inhibitor and with a 2.0g/l concentration of TPI inhibitor solution is displayed in SEM image of Figure 7. Figure 7a shows the SEM image of as-polished Q235 carbon steel before the corrosion experiment which presented a finely polished steel surface without sodium and potassium. There are some minor scratches and parallel grinding marks that can be formed during the polishing process. Figure 7b shows the SEM image of corroded Q235 carbon steel in an inhibitor-free simulated concrete pore solution, indicating rough surface of highly corroded steel and there are full of deep pits and cavities which crated from the aggressive attack of ions in simulated concrete pore solution. On the other hand, Figure 7c exhibits an SEM image of Q235 carbon steel in a simulated concrete pore solution that contains 2.0 g/l concentration of TPI. It depicts a very smooth surface of steel which appears very similar to that of as-polished steel surface in Figure 7a. This reveals that a protective film is formed by the inhibitor molecules on the carbon steel surface which

retards the attack of the Cl^- species and inhibits remarkably the corrosion of carbon steel in simulated-concrete-pore solution.

4. CONCLUSION

This paper is an electrochemical investigation of TPI as a natural corrosion inhibitor for Q235 carbon steel in simulated concrete pore solution. TPI or gutta-percha was extracted from Eucommia bark and leaves and used as a corrosion inhibitor in electrochemical corrosion studies. EIS and polarization measurements revealed enhanced corrosion resistance of Q235 carbon steel in addition to the TPI in corrosive media. Results showed that the maximum values of corrosion inhibition efficiency were obtained at an average of 85.48% for Q235 carbon steel in a simulated concrete pore solution that contains 3.5wt% NaCl and 2.0g/L concentration of TPI. Results of the study into the surface morphology of steel revealed that a protective film was formed by the inhibitor molecules on the carbon steel surface which retarded the attack of the Cl^- species and inhibited remarkably the corrosion of carbon steel in simulated-concrete-pore solution.

References

1. I. Adejuyigbe, P.C. Chiadighikaobi and D.A. Okpara, *Civil Engineering Journal*, 5 (2019) 172.
2. L. Sun, C. Li, C. Zhang, Z. Su and C. Chen, *International Journal of Structural Stability and Dynamics*, 18 (2018) 1840001.
3. S. Taheri, *Construction and Building Materials*, 204 (2019) 492.
4. H. Huang, M. Huang, W. Zhang and S. Yang, *Structure and infrastructure engineering*, 17 (2021) 1210.
5. W. Liu, Z. Guo, C. Wang and S. Niu, *Construction and Building Materials*, 299 (2021) 124011.
6. J. Feng, B. Chen, W. Sun and Y. Wang, *Construction and Building Materials*, 280 (2021) 122460.
7. S. Kakooei, H.M. Akil, M. Jamshidi and J. Rouhi, *Construction and Building Materials*, 27 (2012) 73.
8. Z. Chen and H. Ye, *Cement and Concrete Research*, 143 (2021) 106398.
9. W. Zhang and Z. Tang, *Journal of Composites for Construction*, 25 (2021) 04021043.
10. R. Zhao, L. Zhang, B. Guo, Y. Chen, G. Fan, Z. Jin, X. Guan and J. Zhu, *Composites Part B: Engineering*, 222 (2021) 109092.
11. K. Tan, Y. Qin, T. Du, L. Li, L. Zhang and J. Wang, *Construction and Building Materials*, 287 (2021) 123078.
12. S. Hooshmand Zaferani, M. Sharifi, D. Zaarei and M.R. Shishesaz, *Journal of Environmental Chemical Engineering*, 1 (2013) 652.
13. H. Xu, X.-Y. Wang, C.-N. Liu, J.-N. Chen and C. Zhang, *Soil and Tillage Research*, 212 (2021) 105074.
14. Y.P. Asmara, T. Kurniawan, A.G.E. Sutjipto and J. Jafar, *Indonesian Journal of Science and Technology*, 3 (2018) 158.
15. B. Huang, L. Changhe, Y. Zhang, D. Wenfeng, Y. Min, Y. Yuying, Z. Han, X. Xuefeng, W. Dazhong and S. Debnath, *Chinese Journal of Aeronautics*, 34 (2021) 1.

16. D. She, J. Dong, J. Zhang, L. Liu, Q. Sun, Z. Geng and P. Peng, *Composites Science and Technology*, 175 (2019) 1.
17. Z. Duan, C. Li, W. Ding, Y. Zhang, M. Yang, T. Gao, H. Cao, X. Xu, D. Wang and C. Mao, *Chinese journal of mechanical engineering*, 34 (2021) 1.
18. S. Kakooei, H.M. Akil, A. Dolati and J. Rouhi, *Construction and Building Materials*, 35 (2012) 564.
19. G. Cui, Z. Liu, M. Wei and L. Yang, *Industrial Crops and Products*, 121 (2018) 142.
20. F.R. Shan, M.Q. Wang, Y. Bai and Z.M. Yu, *Advanced Materials Research*, 236 (2011)
21. M.A. Baltazar-Zamora, D. M Bastidas, G. Santiago-Hurtado, J.M. Mendoza-Rangel, C. Gaona-Tiburcio, J.M. Bastidas and F. Almeraya-Calderón, *Materials*, 12 (2019) 4007.
22. P. Xu, J. Zhou, G. Li, P. Wang, P. Wang, F. Li, B. Zhang and H. Chi, *Construction and Building Materials*, 288 (2021) 123101.
23. P. Bocchetta, L.-Y. Chen, J.D.C. Tardelli, A.C.d. Reis, F. Almeraya-Calderón and P. Leo, *Coatings*, 11 (2021) 487.
24. N. Velazquez-Torres, J. Porcayo-Calderon, H. Martinez-Valencia, R. Lopes-Cecenes, I. Rosales-Cadena, E. Sarmiento-Bustos, C.I. Rocabruno-Valdés and J.G. Gonzalez-Rodriguez, *Coatings*, 11 (2021) 1136.
25. R. Solmaz, G. Kardaş, B. Yazıcı and M. Erbil, *Colloids and Surfaces A: Physicochemical and Engineering Aspects*, 312 (2008) 7.
26. L. Valek, S. Martinez, D. Mikulić and I. Brnardić, *Corrosion Science*, 50 (2008) 2705.
27. Y. Wang, Y. Zuo, X. Zhao and S. Zha, *Applied Surface Science*, 379 (2016) 98.
28. A. Singh, Y. Caihong, Y. Yaocheng, N. Soni, Y. Wu and Y. Lin, *ACS omega*, 4 (2019) 3420.
29. M. Liu, C. Li, Y. Zhang, Q. An, M. Yang, T. Gao, C. Mao, B. Liu, H. Cao and X. Xu, *Frontiers of Mechanical Engineering*, 16 (2021) 649.
30. L. Jinsong, G. Qian, L. Jing and F. Lin, *International Journal of Electrochemical Science*, 17 (2022) 22027.
31. N. Naderi, M. Hashim, J. Rouhi and H. Mahmodi, *Materials science in semiconductor processing*, 16 (2013) 542.
32. H. Yang, W. Li, X. Liu, A. Liu, P. Hang, R. Ding, T. Li, Y. Zhang, W. Wang and C. Xiong, *Construction and Building Materials*, 225 (2019) 90.
33. J. Tan, L. Guo, H. Yang, F. Zhang and Y. El Bakri, *RSC Advances*, 10 (2020) 15163.
34. R. Mohamed, J. Rouhi, M.F. Malek and A.S. Ismail, *International Journal of Electrochemical Science*, 11 (2016) 2197.
35. J. Grandle and S. Taylor, *Corrosion*, 50 (1994) 792.
36. M. Liu, C. Li, C. Cao, L. Wang, X. Li, J. Che, H. Yang, X. Zhang, H. Zhao and G. He, *Food Engineering Reviews*, 13 (2021) 822.
37. C. Ogukwe, C. Akalezi, M. Chidiebere, K. Oguzie, Z. Iheabunike and E. Oguziea, *Portugaliae Electrochimica Acta*, 30 (2012) 189.
38. Y.-M. Chu, U. Nazir, M. Sohail, M.M. Selim and J.-R. Lee, *Fractal and Fractional*, 5 (2021) 119.
39. A.K. Singh and M. Quraishi, *International Journal of Electrochemical Science*, 7 (2012) 3222.
40. A.K. Singh, M. Quraishi and E.E. Ebenso, *International Journal of Electrochemical Science*, 6 (2011) 5676.
41. M. Nazeer, F. Hussain, M.I. Khan, E.R. El-Zahar, Y.-M. Chu and M. Malik, *Applied Mathematics and Computation*, 420 (2022) 126868.
42. D.B. Hmamou, R. Salghi, A. Zarrouk, H. Zarrok, B. Hammouti, S. Al-Deyab, M. Bouachrine, A. Chakir and M. Zougagh, *International Journal of Electrochemical Science*, 7 (2012) 5716.
43. M.A. Amin and M.M. Ibrahim, *Corrosion Science*, 53 (2011) 873.
44. K.F. Khaled and M.A. Amin, *Corrosion Science*, 51 (2009) 1964.
45. C. Andrade and C. Alonso, *Materials and Structures*, 37 (2004) 623.

46. Y.-M. Chu, B. Shankaralingappa, B. Gireesha, F. Alzahrani, M.I. Khan and S.U. Khan, *Applied Mathematics and Computation*, 419 (2022) 126883.
47. E.A. Noor, *International Journal of Electrochemical Science*, 2 (2007) 996.
48. L. Tang, Y. Zhang, C. Li, Z. Zhou, X. Nie, Y. Chen, H. Cao, B. Liu, N. Zhang and Z. Said, *Chinese Journal of Mechanical Engineering*, 35 (2022) 1.
49. B. Praveen and T. Venkatesha, *International Journal of Electrochemical Science*, 4 (2009) 267.
50. C. Xin, L. Changhe, D. Wenfeng, C. Yun, M. Cong, X. Xuefeng, L. Bo, W. Dazhong, H.N. LI and Y. ZHANG, *Chinese Journal of Aeronautics*, (2021) 1.
51. T.H. Zhao, M.I. Khan and Y.M. Chu, *Mathematical Methods in the Applied Sciences*, (2021) 1.
52. H. Badawy, J. Brunellière, M. Veryaskina, G. Brotons, S. Sablé, I. Lanneluc, K. Lambert, P. Marmey, A. Milsted and T. Cutright, *International journal of molecular sciences*, 16 (2015) 4392.
53. D. Zhang, L. Gao and G. Zhou, *Corrosion*, 61 (2005) 392.
54. Y. Zhang, H.N. Li, C. Li, C. Huang, H.M. Ali, X. Xu, C. Mao, W. Ding, X. Cui and M. Yang, *Friction*, (2022) 1.
55. C Jing, B.Q.Dong,A. Raza, T.J Zhang,Y.X.Zhang, *Nano Materials Science*,3(2021)47.